



Contents lists available at ScienceDirect

Infrared Physics & Technology

journal homepage: www.elsevier.com/locate/infrared

Demonstration of a bias tunable quantum dots-in-a-well focal plane array

Jonathan Andrews^{a,b,*}, Woo-Yong Jang^a, Jorge E. Pezoa^a, Yagya D. Sharma^a, Sang Jun Lee^c, Sam Kyu Noh^c, Majeed M. Hayat^a, Sergio Restaino^b, Scott W. Teare^d, Sanjay Krishna^a^a ECE Dept. and Center for High Technology Materials, Univ. of New Mexico, Albuquerque, NM 87106, United States^b Naval Research Laboratory, Remote Sensing Division, Code 7216, Albuquerque, NM 87117, United States^c Korea Research Institute of Standards and Science, Daejeon, Republic of Korea^d Electrical Engineering Dept., New Mexico Tech, Socorro, NM 87801, United States

ARTICLE INFO

Article history:

Available online xxxxx

PACS:

81.07.St

81.07.Ta

81.05.Ea

81.07.–b

85.60.Gz

85.35.Be

Keywords:

Quantum Dots

Quantum Wells

III–V Semiconductors

Photodetectors

Infrared Imaging

Multispectral Imaging

ABSTRACT

Infrared detectors based on quantum wells and quantum dots have attracted a lot of attention in the past few years. Our previous research has reported on the development of the first generation of quantum dots-in-a-well (DWELL) focal plane arrays, which are based on InAs quantum dots embedded in an InGaAs well having GaAs barriers. This focal plane array has successfully generated a two-color imagery in the mid-wave infrared (i.e. 3–5 μm) and the long-wave infrared (i.e. 8–12 μm) at a fixed bias voltage. Recently, the DWELL device has been further modified by embedding InAs quantum dots in InGaAs and GaAs double wells with AlGaAs barriers, leading to a less strained InAs/InGaAs/GaAs/AlGaAs heterostructure. This is expected to improve the operating temperature while maintaining a low dark current level. This paper examines 320×256 double DWELL based focal plane arrays that have been fabricated and hybridized with an Indigo 9705 read-out integrated circuit using Indium-bump (flip-chip) technology. The spectral tunability is quantified by examining images and determining the transmittance ratio (equivalent to the photocurrent ratio) between mid-wave and long-wave infrared filter targets. Calculations were performed for a bias range from 0.3 to 1.0 V. The results demonstrate that the mid-wave transmittance dominates at these low bias voltages, and the transmittance ratio continuously varies over different applied biases. Additionally, radiometric characterization, including array uniformity and measured noise equivalent temperature difference for the double DWELL devices is computed and compared to the same results from the original first generation DWELL. Finally, higher temperature operation is explored. Overall, the double DWELL devices had lower noise equivalent temperature difference and higher uniformity, and worked at higher temperature (70 K and 80 K) than the first generation DWELL device.

Published by Elsevier B.V.

1. Introduction

The use of infrared focal plane arrays for thermal imaging, night vision, satellite imaging, distance ranging and improvised explosive device detection has been ongoing for both military and commercial applications [1–4]. Established technologies in both HgCdTe [5] and quantum well infrared photodetectors (QWIPs) with various doping and impurities have produced FPAs capable of detection across much of the infrared spectrum from mid-wave ($\sim 4 \mu\text{m}$) to very long-wave ($24 \mu\text{m} +$) [1,6–8]. Previous research in a hybrid between the QWIP and the QDIP, called the dot-in-a-well, or DWELL, was proposed recently and its performance has been

demonstrated in the literature [9,10]. Advantages of the DWELL structure include multi-spectral response with a bias-dependent spectral tuning [11]. More recently, the DWELL structure has been modified by embedding quantum dots (QDs) in a quantum well (QW) and then embedding this structure within another QW [12]. This new structure has the advantage of lower strain in the heterostructure, which leads to higher temperature operation while maintaining low dark current. Comparison of the bias tunability of these structures and their performance at various device temperatures will validate the performance increase of these new double DWELL structures.

2. DWELL detector structure

The DWELL structure is composed of an active region (15 layers) of n-doped InAs QDs embedded in an $\text{In}_{0.15}\text{Ga}_{0.85}\text{As}$ QW with GaAs barriers, creating an InAs/InGaAs/GaAs heterostructure. The more

* Corresponding author. Address: Naval Research Laboratory, Remote Sensing Division, Code 7216, c/o AFRL, 3550 Aberdeen Ave SE, Albuquerque, NM 87117, United States. Tel.: +1 505 846 6037; fax: +1 505 846 2212.

E-mail address: jonathan.andrews@kirtland.af.mil (J. Andrews).

Report Documentation Page		Form Approved OMB No. 0704-0188
Public reporting burden for the collection of information is estimated to average 1 hour per response, including the time for reviewing instructions, searching existing data sources, gathering and maintaining the data needed, and completing and reviewing the collection of information. Send comments regarding this burden estimate or any other aspect of this collection of information, including suggestions for reducing this burden, to Washington Headquarters Services, Directorate for Information Operations and Reports, 1215 Jefferson Davis Highway, Suite 1204, Arlington VA 22202-4302. Respondents should be aware that notwithstanding any other provision of law, no person shall be subject to a penalty for failing to comply with a collection of information if it does not display a currently valid OMB control number.		
1. REPORT DATE 2009	2. REPORT TYPE	3. DATES COVERED 00-00-2009 to 00-00-2009
4. TITLE AND SUBTITLE Demonstration of a bias tunable quantum dots-in-a-well focal plane array		5a. CONTRACT NUMBER
		5b. GRANT NUMBER
		5c. PROGRAM ELEMENT NUMBER
6. AUTHOR(S)	5d. PROJECT NUMBER	
	5e. TASK NUMBER	
	5f. WORK UNIT NUMBER	
7. PERFORMING ORGANIZATION NAME(S) AND ADDRESS(ES) University of New Mexico, Department of Electrical and Computer Engineering, Center for High Technology Materials, Albuquerque, NM, 87106		8. PERFORMING ORGANIZATION REPORT NUMBER
9. SPONSORING/MONITORING AGENCY NAME(S) AND ADDRESS(ES)		10. SPONSOR/MONITOR'S ACRONYM(S)
		11. SPONSOR/MONITOR'S REPORT NUMBER(S)
12. DISTRIBUTION/AVAILABILITY STATEMENT Approved for public release; distribution unlimited		
13. SUPPLEMENTARY NOTES		
14. ABSTRACT Infrared detectors based on quantum wells and quantum dots have attracted a lot of attention in the past few years. Our previous research has reported on the development of the first generation of quantum dots-in-a-well (DWELL) focal plane arrays, which are based on InAs quantum dots embedded in an InGaAs well having GaAs barriers. This focal plane array has successfully generated a two-color imagery in the mid-wave infrared (i.e. 3?5 lm) and the long-wave infrared (i.e. 8?12 lm) at a fixed bias voltage. Recently, the DWELL device has been further modified by embedding InAs quantum dots in InGaAs and GaAs double wells with AlGaAs barriers, leading to a less strained InAs/InGaAs/GaAs/AlGaAs heterostructure. This is expected to improve the operating temperature while maintaining a low dark current level. This paper examines 320 256 double DWELL based focal plane arrays that have been fabricated and hybridized with an Indigo 9705 read-out integrated circuit using Indium-bump (flip-chip) technology. The spectral tunability is quantified by examining images and determining the transmittance ratio (equivalent to the photocurrent ratio) between mid-wave and long-way infrared filter targets. Calculations were performed for a bias range from 0.3 to 1.0 V. The results demonstrate that the mid-wave transmittance dominates at these low bias voltages, and the transmittance ratio continuously varies over different applied biases. Additionally, radiometric characterization, including array uniformity and measured noise equivalent temperature difference for the double DWELL devices is computed and compared to the same results from the original first generation DWELL. Finally, higher temperature operation is explored. Overall, the double DWELL devices had lower noise equivalent temperature difference and higher uniformity, and worked at higher temperature (70 K and 80 K) than the first generation DWELL device.		
15. SUBJECT TERMS		

16. SECURITY CLASSIFICATION OF:			17. LIMITATION OF ABSTRACT Same as Report (SAR)	18. NUMBER OF PAGES 5	19a. NAME OF RESPONSIBLE PERSON
a. REPORT unclassified	b. ABSTRACT unclassified	c. THIS PAGE unclassified			

recent double DWELL (DDWELL) structure was accomplished in two steps called the intermediate DDWELL and the complete DDWELL. Both devices are again composed of InAs QDs (30 layers) embedded in an $\text{In}_{0.15}\text{Ga}_{0.85}\text{As}$ QW, but this time the entire structure is embedded in another GaAs QW with $\text{Al}_{0.10}\text{Ga}_{0.90}\text{As}$ barriers creating an InAs/InGaAs/GaAs/AlGaAs heterostructure. These band structures of each device are shown in Fig. 1. An intermediate DDWELL was developed to explore the benefits of this structure over the more symmetric complete DDWELL. The larger number of active layers with the DDWELL structures is possible because of the lower strain within the heterostructure. The spectral response for single a single pixel detector DDWELL device is demonstrated in Fig. 2 and can be compared to that of the DWELL device in previous work [10,12,13].

The DWELL and DDWELL samples reported here was grown using molecular beam epitaxy and processed using a standard indium bump flip-chip technique into a 320×256 detector matrix at the University of New Mexico [14]. Each of the detector matrices was then hybridized (by Qmagiq, LLC) to an Indigo Systems Corporation ISC9705 read-out circuit. After hybridization, the FPA was tested at UNM using CamiRa™ system manufactured by SE-IR Corp.

3. Bias tunable performance

Previous literature on the spectral tunability of these DWELL structures has been reported for single pixel devices [10,12]. These results have shown that the MWIR response dominates at low biases (between -1 V and $+1$ V). As the bias is increased, the LWIR response is eventually intensified. Also the bias-dependent spectral tunability (i.e. spectral shift) based on the quantum confined Stark effect was observed at device temperatures of 60 K, 77 K, and 100 K in both mid-wave infrared (MWIR) and long-wave infrared (LWIR). However, nothing has been published on the bias tunability of the finished focal plan arrays.

Images from the new intermediate DDWELL and complete DDWELL at a 60 K FPA temperature were acquired when observing a calibrated blackbody source through various filters covering the MWIR and LWIR. Five optical filters used have bandwidths of $3\text{--}4\text{ }\mu\text{m}$ (MW_1), $4\text{--}5\text{ }\mu\text{m}$ (MW_2), $7.5\text{--}10.5\text{ }\mu\text{m}$ (LW_1), $7.5\text{--}9.5\text{ }\mu\text{m}$ (LW_2) and $8\text{--}11\text{ }\mu\text{m}$ (LW_3), respectively. Tuning of the response was explored for bias values (between 0.3 and 0.8 V tested for the intermediate DDWELL, between 0.3 and 1.5 V for the complete DDWELL). Larger biases are not available due to the saturation of the integration capacitors in the commercial ROIC. Fig. 3

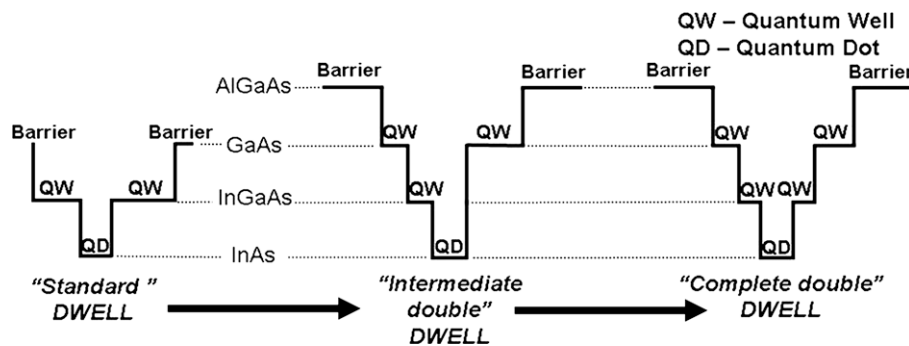


Fig. 1. Progression of structure from DWELL to intermediate double DWELL and finally to complete double DWELL.

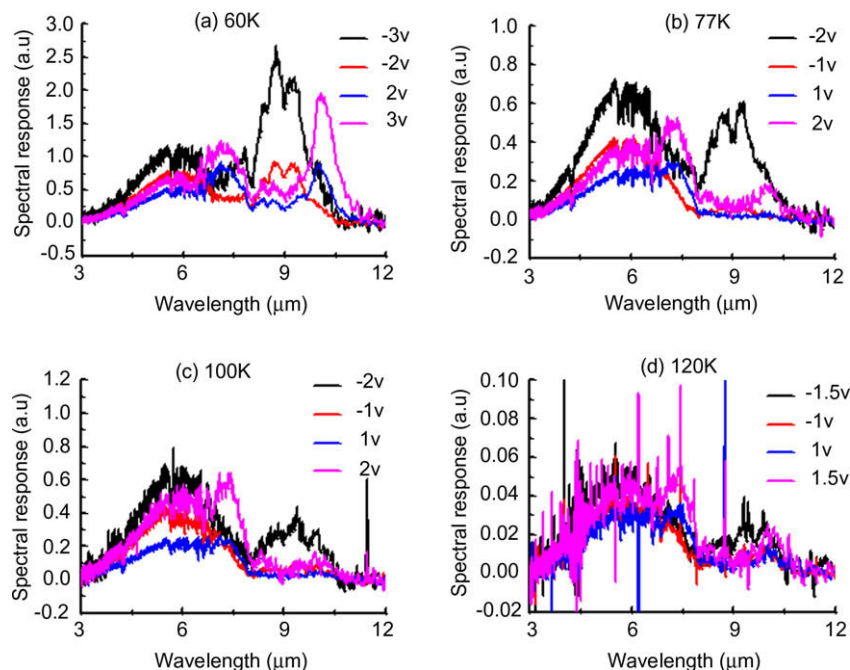


Fig. 2. Bias-dependent spectral responses of “complete” DDWELL for different operating temperatures at (a) 60 K, (b) 77 K, (c) 100 K and (d) 120 K.

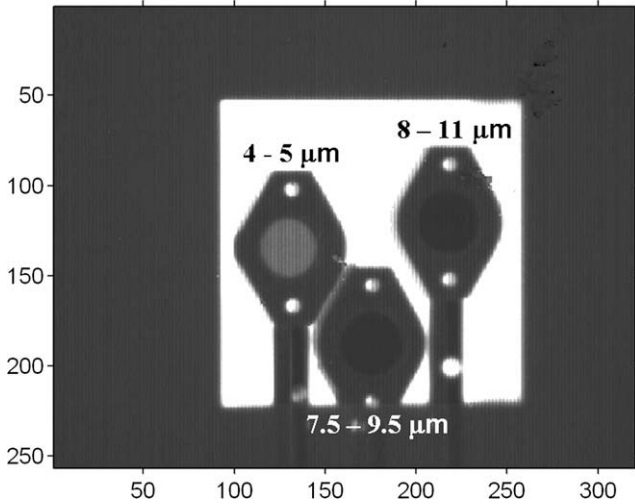


Fig. 3. Non-uniformity corrected image from FPA when imaging blackbody source with three filters.

shows a typical image acquired after non-uniformity correction of the blackbody source and filters. Visual examination of these images yields only small changes in transmitted light through the filters when the bias values are tuned. The images were therefore analyzed to determine the transmittance ratio (equivalent to the photocurrent ratio) between the MWIR and LWIR filter targets. The transmittance ratio was further adjusted by a factor ($Q = \text{ph/cm}^2 \text{ s}$) considering blackbody radiation over wavelengths. The results for both DDWELL devices are described in Tables 1 and 2. The ratio of transmittance change and percentage change

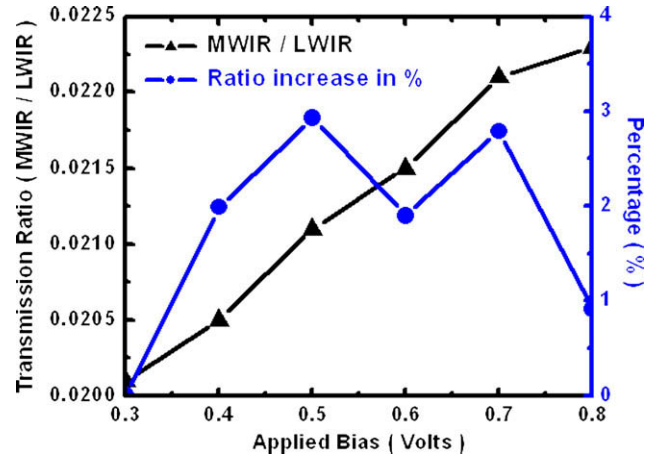


Fig. 4. Adjusted ratio of MWIR to LWIR versus applied bias for MW₁ to LW₁ filters and percentage change.

for DDWELL intermediate are graphed in Fig. 4, while the same results for DDWELL complete are shown in Fig. 5.

Bias-tuning results demonstrate several key points, first, for DDWELL FPAs, the MWIR/LWIR transmittance ratios were varied as larger biases were applied. This is a sign of bias-dependency. In particular, the ratio change of the complete DDWELL FPA in Fig. 5 verifies that more LWIR responses were emerged as applied bias was greater than 0.8 V. It is to be noted that there are overall increases of approximately 11% and 12% in a bias range from 0.3 to 0.8 V for the intermediate DDWELL FPA and the complete DDWELL FPA, respectively. For the complete DDWELL FPA, overall ratio decrease of approximately 10% was obtained for a bias range from 0.8 to 1.5 V.

Table 1

Adjusted ratio of transmittance and percentage change in ratio with applied bias voltage for DDWELL intermediate.

V_{bias} (V)	$Q_{\text{ratio}} \times (\text{MW}_1/\text{LW}_1)$	Ratio change for MW ₁ /LW ₁ (%)	Descriptions
0.3	0.0201	0.00	MW ₁ = Mid-wave filter with a bandwidth of 3–4 μm LW ₁ = Long-wave filter with a bandwidth of 7.5–10.5 μm
0.4	0.0205	1.99	
0.5	0.0211	2.93	
0.6	0.0215	1.9	
0.7	0.0221	2.79	
0.8	0.0223	0.91	
Q_{ratio}	$Q_{\text{MW1}}/Q_{\text{LW1}} = 0.0193$		

Table 2

Adjusted ratio of transmittance and percentage change in ratio with applied bias voltage for DDWELL complete.

V_{bias} (V)	$Q_1 \times (\text{MW}_2/\text{LW}_2)$	$Q_2 \times (\text{MW}_2/\text{LW}_3)$	Ratio change for MW_2/LW_2 (%)	Ratio change for MW_2/LW_3 (%)	Descriptions
0.3	0.1051	0.0663	0.00	0.00	MW_2 = Mid-wave filter with a bandwidth of 4–5 μm
0.4	0.1100	0.0695	4.7	4.86	
0.5	0.1130	0.0713	2.74	2.68	
0.6	0.1172	0.0741	3.70	3.81	
0.7	0.1181	0.0747	0.77	0.88	LW_2 = Long-wave filter with a bandwidth of 7.5–9.5 μm
0.8	0.1181	0.0747	0.00	−0.08	
0.9	0.1163	0.0735	−1.51	−1.50	
1.0	0.1124	0.0721	−3.38	−2.00	
1.1	0.1106	0.0700	−1.59	−2.86	LW_3 = Long-wave filter with a bandwidth of 8.0–11.0 μm
1.2	0.1069	0.0681	−3.38	−2.70	
1.3	0.1071	0.0676	0.21	−0.80	
1.4	0.1064	0.0674	−0.64	−0.30	
1.5	0.1063	0.0673	−0.09	−0.14	
Q_{ratio}	$Q_1 = Q_{\text{MW}2}/Q_{\text{LW}2} = 0.0920$, $Q_2 = Q_{\text{MW}2}/Q_{\text{LW}3} = 0.0579$				

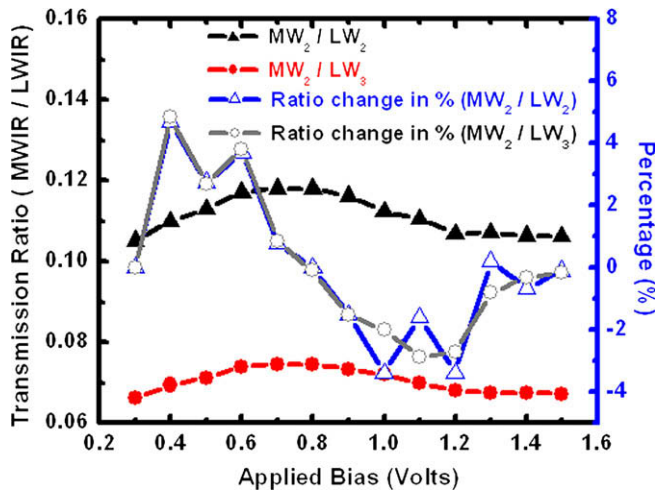


Fig. 5. Adjusted ratio of MWIR to LWIR versus applied bias for MW₂ to LW₂ and LW₃ filters and percentage change.

Table 3

Tabulated results for array averaged NEDT, minimum NEDT array and standard deviation (in Volts).

Device	Parameter (°mK)	60 °K	70 °K	80 °K
DWELL	NEDT	143.0	783.9	N/A
	NEDT min.	107.2	522.7	N/A
	Standard deviation	0.050–0.101	0.092–0.119	N/A
DDWELL I	NEDT	105.7	161.3	389.4
	NEDT min.	78.5	117.1	243.8
	Standard deviation	0.071–0.116	0.064–0.108	0.105–0.131
DDWELL C	NEDT	160.6	167.1	484.1
	NEDT min.	105.6	117.4	288.8
	Standard deviation	0.066–0.098	0.056–0.086	0.149–0.158

4. Device comparison

Measurements of the array uniformity and noise equivalent temperature difference (NEDT) for the DDWELL intermediate and complete were compared to that of the DWELL. The temperature of the calibrated blackbody source was varied and the corresponding illumination values calculated and the device response was measured to determine the overall array uniformity, which is quantified by standard deviation of pixel counts. All measurements here were performed at a part temperature of 60 K using a closed-cycle helium pump dewar. The results for array uniformity are displayed in Table 3.

The minimum NEDT of all devices was measured using the same method of changing the illumination via the blackbody source. The results of the minimum NEDT value on the array at each illumination level is shown in Fig. 6 for the DDWELL intermediate, DDWELL complete and the original DWELL devices.

5. Higher temperature operation

Development of the DDWELL structures was initiated to increase the number of active layers (and thus the responsivity) and explore higher part temperature operation. Infrared camera systems development is often interested in increasing the operational temperature of focal plane arrays to minimize cryogenic cooling requirements to develop smaller overall systems.

The DWELL and DDWELL devices were also operated using the same closed-cycle helium pump dewar at 70 K and 80 K. The re-

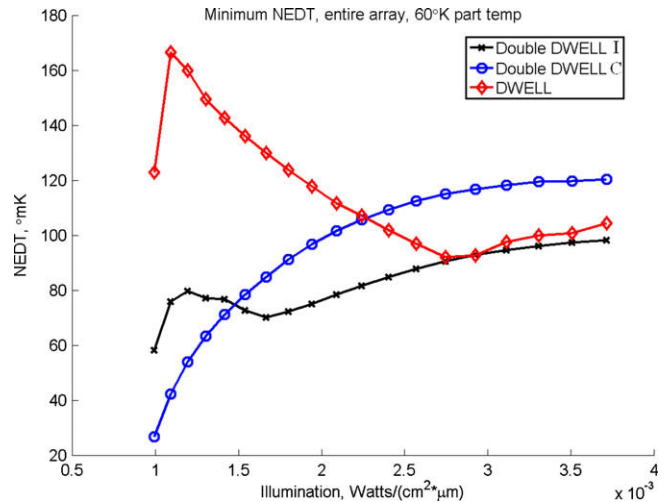


Fig. 6. Minimum NEDT for three devices versus illumination provided by calibrated blackbody.

sults for these tests are shown in Table 3 with the values tabulated for NEDT are computed at an illumination of $2 \times 10^{-3} \text{ W}/(\text{cm}^2 \mu\text{m})$. The DWELL device was inoperable at 80 K and was functional at 70 K, although at very high NEDT showing severely reduced sensitivity. Both DDWELL devices were operable at both 70 K and 80 K.

6. Conclusions

Our group has developed DDWELL focal plane arrays in an effort to reduce lattice strain mismatch and increase temperature of operation while maintaining low noise. When compared to the first generation DWELL structure, the higher temperature operation is evident. At 60 K, all devices performed similarly with around 100 mK NEDT. However, at 70 K the DWELL increased to over 500 mK NEDT while the DDWELLs maintained similar sensitivities. At 80 K, the DWELL was inoperable, and although both DDWELL devices had around 250 mK NEDT, they were still operable. Additionally, the bias tunability of DDWELL FPA was demonstrated by the transmittance ratio compared between MWIR and LWIR outputs. The ratio change has shown the dominance of MW outputs at low applied biases, however, more LW outputs were observed with a bias of 0.8 V or greater. This is significant in terms of realizing the consistent behavior of DDWELL FPA as compared to the bias tunability of its single pixel level.

References

- [1] E.L. Dereniak, G. Boreman, *Infrared Detectors and Systems*, Wiley, New York, 1996 (pp. 2, 30, 298–299, 313–325).
- [2] J.M. Lloyd, *Thermal Imaging Systems*, Plenum, New York, 1975 (p. 3).
- [3] P.A. Jacobs, *Thermal Infrared Characterization of Ground Targets and Backgrounds*, SPIE, vol. TT26, Washington, 1996 (p. 4).
- [4] R.G. Driggers, P. Cox, T. Edwards, *Introduction to Infrared and electro-optical systems*, vol. 85, Artech House, Boston, 1999 (pp. 2–4).
- [5] A. Rogalski, *Opto-Electr. Rev.* 6 (1998) 279–294.
- [6] A. Shen, H.C. Liu, F. Szmulowicz, M. Buchanan, M. Gao, G.J. Brown, J. Ehret, *J. Appl. Phys.* 86 (1999) 5232.
- [7] Z. Chen, E.T. Kim, A. Madhukar, *Appl. Phys. Lett.* 80 (2002) 2490.
- [8] S.D. Gunapala, S.V. Bandara, A. Singh, J.K. Liu, Sir B Rafol, E.M. Luong, J.M. Mumolo, N.Q. Tran, D.Z.-Y. Ting, J.D. Vincent, C.A. Shott, J. Long, P.D. Le Van, *IEEE Trans. Electron. Dev.* 47 (5) (2000) 963.
- [9] E.S. Varley, M. Lenz, S.J. Lee, J.S. Brown, D.A. Ramirez, A. Stintz, S. Krishna, A. Reisinger, M. Sundaram, *Appl. Phys. Lett.* 91 (2007) 081120.
- [10] S. Krishna, D. Forman, S. Annamalai, P. Dowd, P. Varangis, T. Tumolillo Jr., A. Gray, J. Zilko, K. Sun, M. Liu, J. Campbell, D. Carothers, *Appl. Phys. Lett.* (2005) 86.
- [11] S. Krishna, *J. Phys. D* 38 (2005) 2147.

- [12] R.V. Sheno, R.S. Attaluri, J. Shao, Y. Sharma, A. Stintz, T.E. Vandervelde, S. Krishna, Low strain InAs/InGaAs/GaAs/quantum dots-in-a-well infrared photodetector, *J. Vac. Sci. Technol. B* 26 (2008) 1136–1139.
- [13] E.S. Varley, D. Ramirez, J.S. Brown, S.J. Lee, A. Stintz, M. Lenz, S. Krishna, A. Reisinger, M. Sundaram, Demonstration of a two color 320×256 quantum dots-in-a-well focal plane array, *SPIE* 6678 (2007) (OT).
- [14] S. Krishna, S. Raghavan, G. von Winckel, A. Stintz, G. Ariyawansa, S.G. Matsik, A.G.U. Perera, *Appl. Phys. Lett.* 83 (2003) 2746.